This article has been accepted for publication in a future issue of this journal, but has not been fully edited. Content may change prior to final publication. Citation information: DOI 10.1109/TCSVT.2018.2810212, IEEE Transactions on Circuits and Systems for Video Technology

An Adaptive Method for Image Dynamic Range Adjustment

Kai-Fu Yang, Hui Li, Hulin Kuang, Chao-Yi Li, and Yong-Jie Li, *Senior Member, IEEE*

***Abstract*—In this paper, we relate the operation of image dynamic range adjustment to the following two tasks: (1) for a high dynamic range (HDR) image, its dynamic range will be mapped to the available dynamic range of display devices, and (2) for a low dynamic range (LDR) image, its distribution of intensity will be extended to adequately utilize the full dynamic range of display devices. The common goal of the both tasks is to preserve or even enhance the details and improve the visibility of scenes when being matched to the available dynamic range of a display device. In this study, we propose an efficient method for image dynamic range adjustment with three adaptive steps. Firstly, according to the histogram of the luminance map separated from the given RGB image, two suitable Gamma functions are adaptively selected to separately adjust the luminance of the dark and bright components. Secondly, an adaptive fusion strategy is proposed to combine the two adjusted luminance maps in order to balance the enhancement of the details in different regions. Thirdly, an adaptive luminance-dependant color restoration method is designed to combine the fused luminance map with the original color components to obtain more consistent color saturation between the images before and after dynamic range adjustment. Extensive experiments show that the proposed method can efficiently compress the dynamic range of HDR scenes with good contrast, clear details and high structural fidelity of the original image appearance. In addition, the proposed method can also obtain promising performance when being used to enhance LDR nighttime images and greatly facilitate the object (car) detection in nighttime traffic scenes.**

***Index Terms*—HDR rendering, tone mapping, Gamma correction, nighttime image, image enhancement**

I. Introduction

IMAGE dynamic range adjustment is widely used for digital image enhancement. In this work, the operation of image dynamic range adjustment is related to two different tasks: (1) high dynamic range (HDR) rendering or tone mapping, which aims to compress the dynamic range of a HDR image to adapt the available range of the display device for image display, and (2) extending the distribution of intensity to adequately utilize the full dynamic range of the display device and improve the visibility of details when the given scene is of low dynamic range (LDR). It is obvious that these two tasks involve opposite mappings of dynamic range, and in general, a tone mapping method for HDR compression does not work well for LDR extension. The common challenge shared by these two tasks is how to balance the global and local contrasts.

HDR images are usually used to capture more information of natural scenes, because the light intensity in natural scenes of the real world can be as high as in the ratio of 100, 000 to 1. However, most display devices available to us have a limited dynamic range (e.g., 100 to 1) [1]. Therefore, HDR rendering or tone mapping (TM) operators are widely used to reproduce the HDR images to match the limited dynamic range of display devices, so that the details in both the dark and bright areas are as faithfully visible as possible. To achieve this goal, various TM methods have been proposed in recent years. Most TM methods are developed in the spatial domain inspired by the visual adaptation models, while other methods realized in the frequency or gradient domain also exhibit good performance in HDR compression [1].

In details, the spatial-domain based TM methods can be further divided into two categories: global and local operators. Miller *et al*. first introduced the global TM method for dynamic range reduction by keeping the brightness ratio constant [2]. Subsequently, Tumblin and Rushmeier proposed a global operator aiming to preserve the brightness values before and after dynamic range compression [3]. In addition, straightforward logarithmic and exponential mappings also perform well when being applied on the images with dynamic range just higher than LDR of display devices [1]. Drago *et al*. further found that the logarithmic mapping can handle HDR image when adaptively adjusting the base of logarithm according to each pixel's value [4]. On the other hand, by modeling the visual adaption mechanisms, Reinhard and Devlin [5] built a photoreceptor response model for tone mapping according to the well-known Naka-Rushton equation [1], which is used to fit the response curves for both the rods and cones of the biological visual system [6]. Subsequently, more methods were proposed to improve the dynamic range compression based on various modified versions of the photoreceptor response function, such as rational quantization function [7], gain control function [8], S-shaped curve [9], [10], etc. In addition, the threshold versus intensity (TVI) model was also used to match the just-noticeable difference (JND) for dynamic reduction with contrast protection [11]. These global TM operators

Manuscript received June 28, 2017; revised December 28, 2017; accepted February 16, 2018. This work was supported by the Natural Science Foundations of China under Grant 61703075, and the Sichuan Province Science and Technology Support Project under Grant 2017SZ0004, 2017JY0249. The work was also supported by the Fundamental Research Funds for the Central Universities under Grant ZYGX2016KYQD139. *(Corresponding author: Yong-Jie Li)*

K.-F. Yang, H. Li, and Y.-J. Li are with the Clinical Hospital of Chengdu Brain Science Institute, MOE Key Lab for Neuroinformation, University of Electronic Science and Technology of China, Chengdu 610054, China (email:yangkf@uestc.edu.cn, liyj@uestc.edu.cn).

H. Kuang is with the Department of Clinical Neurosciences, University of Calgary, Alberta, Canada. (email:hulinkuang@gmail.com).

C.-Y. Li is with the Clinical Hospital of Chengdu Brain Science Institute, MOE Key Lab for Neuroinformation, University of Electronic Science and Technology of China, Chengdu 610054, China, and the Center for Life Sciences, Shanghai Institutes for Biological Sciences, Chinese Academy of Sciences, Shanghai 200031, China (email:cyli@sibs.ac.cn)

1051-8215 (c) 2018 IEEE. Personal use is permitted, but republication/redistribution requires IEEE permission. See http://www.ieee.org/publications_standards/publications/rights/index.html for more information.

This article has been accepted for publication in a future issue of this journal, but has not been fully edited. Content may change prior to final publication. Citation information: DOI 10.1109/TCSVT.2018.2810212, IEEE Transactions on Circuits and Systems for Video Technology

have the advantages of efficient computation and halo artifact resisting, but may lead to the loss of local contrast [1].

In order to adapt to the local regions instead of the whole scene, local operators have also been developed to adjust each pixels according to the average level over a local neighborhood of each pixel. Among others, based on the Land's Retinex theory [12], Rahman and Jobson developed multiple versions of Retinex implementation for various applications including image enhancement, tone mapping, etc. [13], [14]. Single-scale Retinex (SSR) achieves tone reduction by computing the contrast information in a neighborhood of pixels in the log domain [13]. Subsequently, multi-scale SSR outputs were combined to obtain good dynamic range compression and tonal rendition [14], and color restoration was also introduced in a further version (MSRCR) [14]. In 2006, Meylan *et al*. proposed a novel adaptive Retinex-based method [15], which uses an adaptive filter to the luminance channel for reducing halo artifacts. Lee employed Retinex theory to achieve dynamic range compression and contrast enhancement in the compressed domain [16]. Recently, Gao *et al*. further proposed a luminance-chromaticity independent model to avoid the color distortion in the Meylan's method [17].

There are also many local TM operators that compress the dynamic range based on the photoreceptor response model, but with a blurred version of the image as the local adaptation level. For example, Reinhard *et al*. used the log average luminance to scale the dynamic range and selected an appropriate local scale by center-surround computation to avoid haloing artifacts [5]. Furthermore, some edge-preserving smoothing filters (e.g., Box-shaped filter [18] and bilateral filter [19]) were also used to estimate the local luminance adaptation. The method proposed by Yee *et al*. computed a suitable adaptation level based on the segmentation of bright and dark regions [20]. Recently, Zhang *et al*. built a retina-inspired gap junctional coupling model to select suitable range of local adaptation to avoid halo artifacts [21]. In short, local operators can achieve fine compression in comparison to the global operators, but they are required to carefully estimate suitable adaptation levels for avoiding halo artifacts.

In addition to global and local spatial TM methods, there are some operators compressing the dynamic range of HDR images in the frequency or gradient domain. Frequency-based methods aims to compress the low frequency component and preserve high frequency component [22]. In general, they are based on a simple assumption that HDR images can be separated into illuminant and reflectance, and the illuminant component is of low frequency within an arbitrary HDR while the reflectance component is of typically high frequency and LDR [1]. Durand and Dorsey introduced the bilateral filter to separate the input image into a base layer and a detail layer in the log domain, and the base layer was scaled to reduce the dynamic range. The two layers were then recombined to obtain the compressed image [19]. The subsequent work employed a modified version of bilateral filter called trilateral filter [23]. Besides, guided image filter [24], weighted guided image filter [25] and weighted least squares filters [26] are also widely used to separate a HDR image into a base layer and a detail layer. In addition, there are some works attempting to separate the reflectance from illuminant and compress the dynamic range in the gradient field, such as [27].

On the other hand, there are lots of classical methods aiming to adjust the dynamic range of LDR images. Among others, histogram equalization (HE) and its various modified versions have been widely used for contrast enhancement [28]–[32]. For example, the bi-histogram equalization method [33] independently used HE on two parts of histogram split by the mean value. In order to preserve small details, adaptive histogram equalization was proposed according to the local data [34]. Recently, Rivera *et al*. proposed a content-aware method for dark image enhancement with ad hoc transformation functions for different image regions [35]. Some authors also integrated visual attention into contrast enhancement methods for improving the visual perceptual quality of images [36]–[38] and videos [39].

Some methods that are more related to this work achieve image enhancement by fusing multiple enhanced outputs or multiple resolution images with certain rules. For example, wavelet transform and Laplacian pyramid decomposition were usually used to decompose the input images into multiple scales [40], [41]. Ke *et al.* proposed a bilateral tone adjustment method to enhance the mid-tone regions in addition to the bright and dark regions of the image [38]. In general, fusing multiple images generated by adaptive enhancement can well balance the global and local contrasts and details. There were also some methods attempting to balance the global and local contrasts by finding the optimal tone curves [42], [43].

In this paper, we propose a new dynamic range adjustment method by fusing the results of adaptive Gamma corrections on the luminance component of the input HDR or LDR image, followed by a local enhancement operator. Finally, the RGB image is recovered with a luminance dependent color restoration. From the biological point of view, the proposed idea is inspired from visual adaptation to varying environmental illumination. Firstly, the global visual adaptation is achieved by altering the rod and cone systems in the retina. Under varying environmental illumination, the rod and cone systems in the retina can automatically adjust the irrelative activities to be well adapted to the ambient illumination [44], [45]. In details, rods usually work in the low-light situation, while cones prefer to perceive visual signals under the daylight condition. However, the dynamic range compression usually leads to the loss of local contrast. Therefore, local visual adaptation is necessary to preserve and/or restore the local contrast according to the local magnitude of illuminant. In the visual system, the computational mechanism of dividing normalization is considered as contributing to the local visual adaptation [46], [47]. Inspired by these mechanisms, we employed two adaptive Gamma corrections to handle the global luminance adjustment, and then the local adaptive mechanism contributes to fusing the two globally corrected visual signals. In other words, the local adaptation is achieved by fusing the activities of rods and cones according to the local luminance of visual scenes. In addition, the local normalization also contributes to the detail enhancement with the antagonistic center-surround organization of receptive field.

From the point of view of photograph engineering, our

1051-8215 (c) 2018 IEEE. Personal use is permitted, but republication/redistribution requires IEEE permission. See http://www.ieee.org/publications_standards/publications/rights/index.html for more information.

This article has been accepted for publication in a future issue of this journal, but has not been fully edited. Content may change prior to final publication. Citation information: DOI 10.1109/TCSVT.2018.2810212, IEEE Transactions on Circuits and Systems for Video Technology

proposed idea is more directly inspired by the most common way of generating HDR images in digital cameras for a scene under greatly varying irradiance, i.e., taking multiple LDR images of a scene with different exposures and then fusing them into a HDR image with, for example, a weighted linear summation [48]–[50]. With the similar goal as other HDR tone mapping methods, our method aims to render the captured HDR and LDR images when no multi-exposure images are available. Recently, a more related algorithm was proposed to brighten single image [51], [52]. In that method, three virtual differently exposed images are firstly generated from the input LDR image with an ad hoc global transform, and then the brightened images are fused via a multi-scale algorithm. In contrast, we select two adaptive Gamma curves to produce the intermediate images and fuse the corrected images with a single-scale algorithm. The proposed method is quite simple yet efficient for the both tasks of HDR compression and LDR image enhancement. Our idea can be summarized as the computationally adaptive generation of two-exposure images for the input HDR or LDR image, followed by an adaptive fusion and color restoration.

The main contributions of this work can be summarized in several aspects: (1) a new method is designed to adaptively select two Gamma curves for the global corrections of dark and bright regions, which can well enhance the details in both of the dark and bright regions. The proposed method is available for the two tasks of HDR compression and LDR image enhancement. (2) a single-scale adaptive fusion strategy is proposed to combine the outputs of the two global Gamma corrections for dark and bright regions, which can well balance the enhancement of the details in different regions. (3) an adaptive luminance-dependant color restoration method is designed, which helps obtain more consistent color saturation between the images before and after dynamic range adjustment. Comprehensive experiments show that compared to the state-of-the-art methods, the proposed method can well handle the both tasks of HDR tone mapping and LDR image enhancement.

The rest of the paper is organized as follows. The implementation of our dynamic range adjustment method is described in Section II. The experimental results and the comparisons are presented in Section III. Finally, the conclusion and discussion are summarized in Section IV.

II. Dynamic Range Adjustment Method

Gamma transformation is widely used to adjust the dynamic range of images for contrast enhancement. However, selecting an appropriate parameter of Gamma function is important for a specific image or a specific region of the image. For example, a small Gamma value (< 1) is useful to brighten the dark regions of scenes, while a larger Gamma value (> 1) is suitable for the contrast enhancement of the over-exposed regions. In order to preserve the details in both the under-exposed and over-exposed regions of the image, we proposed a novel method in this paper for dynamic range adjustment by fusing two corrected maps with adaptive Gamma functions according to the histogram of the luminance distribution.

The flowchart of the proposed method is shown in Fig.1. Firstly, we separate the luminance and chromaticity components into independent channels to preserve the color of the original image. The luminance channel is compressed to achieve normalization with a logarithmic transformation. Then two appropriate Gamma transformation functions are adaptively selected according to the gray value distribution of the original luminance channel, and are applied respectively to adjust the dynamic range of dark and bright regions of the input image. The Gamma corrected images are further enhanced by a local operator and then adaptively fused into a unified luminance map with the guidance of local brightness. Finally, the fused luminance image is transformed to the RGB space with an adaptive luminance-dependent color saturation restoration.

A. Logarithmic normalization

For a color image, dynamic range mainly influences the luminance information. Therefore, keeping the color information consistent during the processing of dynamic range adjustment is important for visual naturalness. In this work, we separate the luminance and chromaticity information by transforming the image from RGB space to YC_BC_R space, which is part of various broadcast standards [1]. The Y component of YC_BC_R space is the luminance information, which is defined as

$$L_{in}(x,y) = 0.299 \cdot I_{in}^R(x,y) + 0.587 \cdot I_{in}^G(x,y) + 0.114 \cdot I_{in}^B(x,y) \quad (1)$$

where I_{in}^R, I_{in}^G, and I_{in}^B represent the intensities of the red, green and blue channels of the input image, respectively.

For various given scenes, their dynamic ranges may vary largely. In order to avoid the inconsistent dynamic ranges of input images, a logarithm transform is used to non-linearly normalize the luminance channel as:

$$L_{\log}(x,y) = \log_{\alpha}(L_{in}(x,y) + 1) \quad (2)$$

where we set $\alpha = max(L_{in}(x,y)) + 1$ to adapt various dynamic ranges of input scenes, thus the luminance range of $L_{\log}$ is nonlinearly compressed to the range of 0 to 1.

B. Adaptive Gamma correction

Gamma correction is widely used for dynamic range adjustment. A general formulation of Gamma correction can be written as

$$I_{out}(x,y) = (I_{in}(x,y))^{\gamma} \quad (3)$$

where I_{in} and I_{out} are the input and output images, respectively. It is clear to see that with a small γ value ($\gamma < 1$), the Gamma transform is benefit of improving the brightness and contrast of dark regions in the images, but the bright pixels may be clipped; in contrast, a large γ value ($\gamma > 1$) can recover the details of the over-exposed regions, but the dark regions may be invisible. These characteristics of Gamma transform can be easily found from the Gamma transform curves with different parameters (shown in Fig. 2). In order to obtain a well matched dynamic range of the given image, the key point is to select appropriate parameter (γ) adapting to different scenes or different regions of the given scene.

1051-8215 (c) 2018 IEEE. Personal use is permitted, but republication/redistribution requires IEEE permission. See http://www.ieee.org/publications_standards/publications/rights/index.html for more information.

This article has been accepted for publication in a future issue of this journal, but has not been fully edited. Content may change prior to final publication. Citation information: DOI 10.1109/TCSVT.2018.2810212, IEEE Transactions on Circuits and Systems for Video Technology

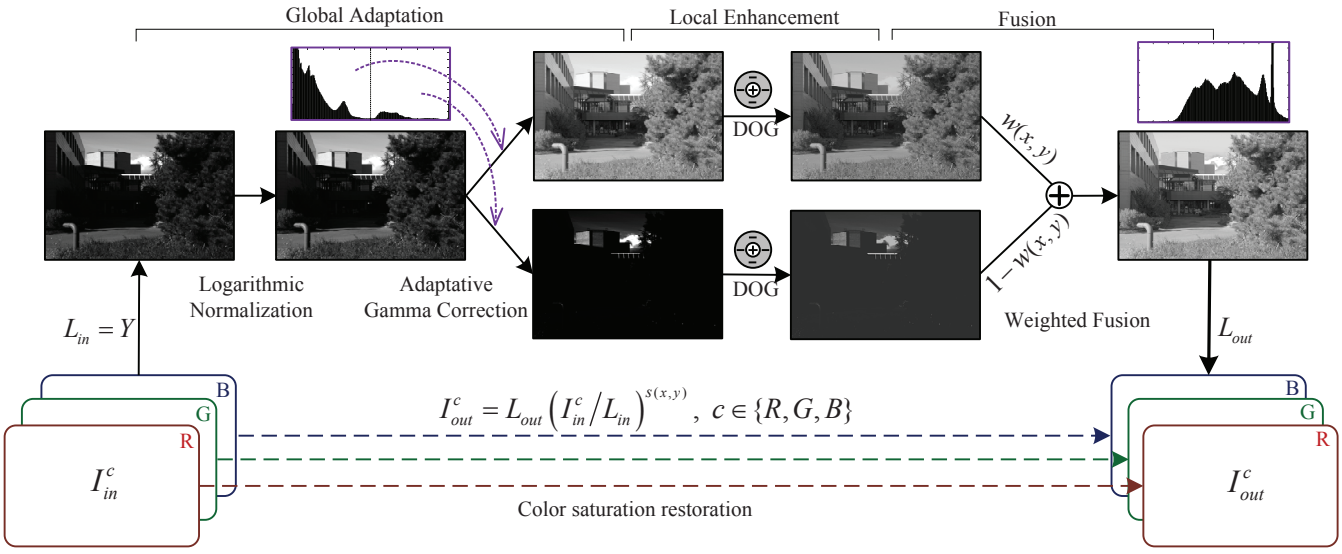

Fig. 1. The flowchart of the proposed dynamic range adjustment method. $w(x,y)$ is computed with (14) and $s(x,y)$ is obtained by using (16).

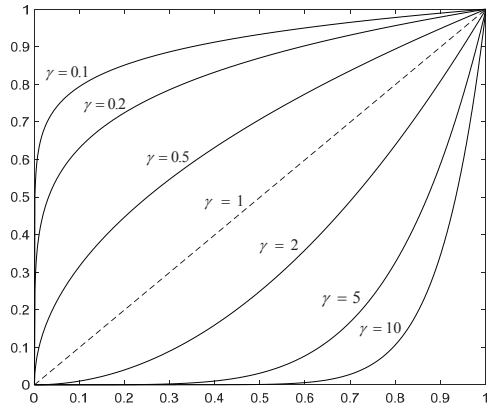

Fig. 2. Various Gamma transformation curves with different γ values.

In this work, we propose a novel strategy for automatic Gamma parameter selection based on the luminance histogram. For the luminance component of the given image, we select two different Gamma transform curves to enhance respectively the dark and bright regions of the same image, considering that an image usually contains under-exposed and over-exposed regions, especially in HDR scenes. Specifically, for the logarithmically normalized luminance channel ($L_{\log}$ with the value range of 0 to 1), we first subdivide the histogram into two parts with a threshold of 0.5, and use σ_L and σ_H to denote the standard deviations of pixels within the dark set (i.e., pixels with $L_{\log}(x,y) \leq 0.5$) and bright set (i.e., pixels with $L_{\log}(x,y) > 0.5$), respectively. Then we set two expected median values of the pixel distribution in the dark and bright sets in the corrected image as

$$M_L = \frac{1}{3} + \sigma_L \tag{4}$$

$$M_H = 1 - \sigma_H \tag{5}$$

Note that we select 1/3 and 1 in (4) and (5) as the bases of the two expected medians, while σ_L and σ_H are used to adaptively fine-tune the expected medians according to the given histogram. This setting is based on the assumption that the predominant pixels are dark in HDR scenes and night images, and this setting can be easily determined when executing different visual tasks.

For convenient description, we use $S^{\gamma_i}_{dark}$ to denote the pixel set with the values lower than 0.5 (i.e., $S^{\gamma_i}_{dark}$ is the pixels with $(L_{\log}(x,y))^{\gamma_i} \leq 0.5$) in the image corrected with γ_i, while $S^{\gamma_i}_{bright}$ to denote the pixel set with the values higher than 0.5 (i.e., $S^{\gamma_i}_{bright}$ is the pixels with $(L_{\log}(x,y))^{\gamma_i} > 0.5$). Then the expected parameters are determined by searching the possible range of γ_i as

$$\gamma_L = \underset{\gamma_i}{arg\,min}\left(|med(S^{\gamma_i}_{dark}) - M_L|\right), \gamma_i \in \{0.1, 0.11, ..., 1\} \tag{6}$$

$$\gamma_H = \underset{\gamma_i}{arg\,min}\left(|med(S^{\gamma_i}_{bright}) - M_H|\right), \gamma_i \in \{1, 1.1, ..., 10\} \tag{7}$$

where $med(S)$ denotes the operator of computing the median value of the pixel set S.

Then we can obtain the images adjusted by Gamma correction with the selected parameters as

$$L_d(x,y) = (L_{\log}(x,y))^{\gamma_L} \tag{8}$$

$$L_b(x,y) = (L_{\log}(x,y))^{\gamma_H} \tag{9}$$

It is obvious that the details in the dark and bright regions of the image become more visible in the Gamma corrected image $L_d(x,y)$ and $L_b(x,y)$, respectively.

1051-8215 (c) 2018 IEEE. Personal use is permitted, but republication/redistribution requires IEEE permission. See http://www.ieee.org/publications_standards/publications/rights/index.html for more information.

This article has been accepted for publication in a future issue of this journal, but has not been fully edited. Content may change prior to final publication. Citation information: DOI 10.1109/TCSVT.2018.2810212, IEEE Transactions on Circuits and Systems for Video Technology

C. Local enhancement and adaptive fusion

Global compression of dynamic range may reduce the local contrast of some regions. Therefore, a local contrast operator is required to recover the image details. Here we use a difference of Gaussian (DoG) filter to enhance the details of Gamma corrected images according to

$$L'_d(x,y) = L_d(x,y) + (L_d * DoG_{\sigma_c,\sigma_s})(x,y) \tag{10}$$

$$L'_b(x,y) = L_b(x,y) + (L_b * DoG_{\sigma_c,\sigma_s})(x,y) \tag{11}$$

$$DoG_{\sigma_c,\sigma_s}(x,y) = \frac{1}{2\pi\sigma_c^2} exp\left(-\frac{x^2+y^2}{2\sigma_c^2}\right) - \frac{1}{2\pi\sigma_s^2} exp\left(-\frac{x^2+y^2}{2\sigma_s^2}\right) \tag{12}$$

where $*$ denotes the convolution operator. In this paper, we set $\sigma_c = 0.5$ and $\sigma_s = 3\sigma_c$ to obtain a small DoG filter for detail enhancement.

It is clear that according to the role of Gamma correction, $L'_d(x,y)$ will provide good contrast in the dark regions, while $L'_b(x,y)$ will preserve the details in bright regions of the input image. Here we design an adaptive luminance-dependant fusion method to integrate the two enhanced images for dynamic range adjustment and contrast enhancement. The final fused map is obtained with

$$L_{out}(x,y) = w(x,y)\cdot L'_d(x,y) + (1-w(x,y))\cdot L'_b(x,y) \tag{13}$$

where $w(x,y)$ is a spatially varying weight, which controls the portion of $L'_d(x,y)$ and $L'_b(x,y)$ to balance the brightness levels of different locations. $w(x,y)$ is given by

$$w(x,y) = \exp\left(-\frac{L_b(x,y)^2}{2{\sigma_w}^2}\right) \tag{14}$$

where we set $\sigma_w = 0.5$ in this paper. (13) and (14) indicate that the fused image $L_{out}(x,y)$ emphasizes simultaneously the enhanced details of bright regions provided in $L'_b(x,y)$ and the details of the dark regions provided in $L'_d(x,y)$.

Finally, in order to balance the local contrast in dark regions and the global contrast during the luminance compression, $L_{out}(x,y)$ is firstly clipped to remove some sparse pixels with the values that are negative or greater than 1, and a linear normalization operator following the pixel-clipping is utilized to scale the dynamic range of compressed luminance to occupy the full 8-bit range.

D. Adaptive color saturation restoration

Tone mapping algorithms often cause color shift (over-saturated or under-saturated), and thus it is necessary to add a color correction step to preserve color appearance after dynamic range compression. Although there are many methods which are proposed for general color correction [53]–[55], as indicated by previous works [1], [7], [56], keeping the ratio between the color channels before and after dynamic range adjustment constant is a simple and efficient way for reducing the color shift when recombining luminance values into a color image. A common method of controlling the saturation of color is suggested as (15) but with a fixed exponent s in the literature [1]. As indicated by [57], this equation may also introduce undesirable luminance shift. Therefore, a possible strategy for color appearance preservation is to estimate luminance-dependant s for each given HDR scene. Mantiuk *et al*. have provided a sigmoid function to compute the parameter s depending on the contrast compression factor, which can fit the data of subjective study well [57]. However, such function introduces two extra parameters and needs to estimate the contrast compression factor firstly.

In our work, we combine two Gamma corrected images for luminance compression according to local luminance, which results in the difficulty of exactly estimating the contrast compression factor. Alternatively, we design a simple luminance-dependent function for s estimate, considering that the greater compression often happens in the dark regions during the mapping. It is also based on a simple observation that higher saturation in the bright regions of image will appear in dazzling. Therefore, we attenuate the saturation of pixels with high brightness by reducing the exponent s. The final processed color image $I^c_{out}(x,y)$ is obtained as

$$I^c_{out}(x,y) = L_{out}(x,y)\left(\frac{I^c_{in}(x,y)}{L_{in}(x,y)}\right)^{s(x,y)} \tag{15}$$

$$s(x,y) = 1 - \tanh(L_b(x,y)) \tag{16}$$

where $c \in \{R,G,B\}$, s decreases with the increasing of luminance $L_b(x,y)$, and the $tanh(\cdot)$ function is used to constrain the minimum of s to avoid excessive under-saturation. From the results shown in Section III (Fig. 4), the proposed luminance-dependent function can efficiently reduce the color shift in a parameter free way.

III. Experimental Results

In this section, we will first demonstrate the basic adaptive properties of the proposed method, including adaptive Gamma correction and adaptive color saturation restoration. Furthermore, we will evaluate our method on two dynamic range adjustment tasks: (1) dynamic range compression or tone mapping for HDR scenes, and (2) night image (LDR image) enhancement and its application in car detection in night traffic scenes.

A. Adaptive properties of the proposed method

The most important property of our method is the adaptive selection of optimal Gamma curves for the given scenes. Fig.3 shows two examples of adaptive Gamma correction. The image in the top row has predominant dark regions and a few of over-bright pixels (e.g., the light on the right-up corner), thus a Gamma curve with smaller γ (red curve) is selected to improve the brightness level of dark regions and a Gamma curve with higher γ (blue curve) is selected to recover the details in bright regions. On the other hand, with an over-exposed scene (bottom row), our method select a Gamma curve with higher γ (blue curve) to improve the visibility

1051-8215 (c) 2018 IEEE. Personal use is permitted, but republication/redistribution requires IEEE permission. See http://www.ieee.org/publications_standards/publications/rights/index.html for more information.

This article has been accepted for publication in a future issue of this journal, but has not been fully edited. Content may change prior to final publication. Citation information: DOI 10.1109/TCSVT.2018.2810212, IEEE Transactions on Circuits and Systems for Video Technology

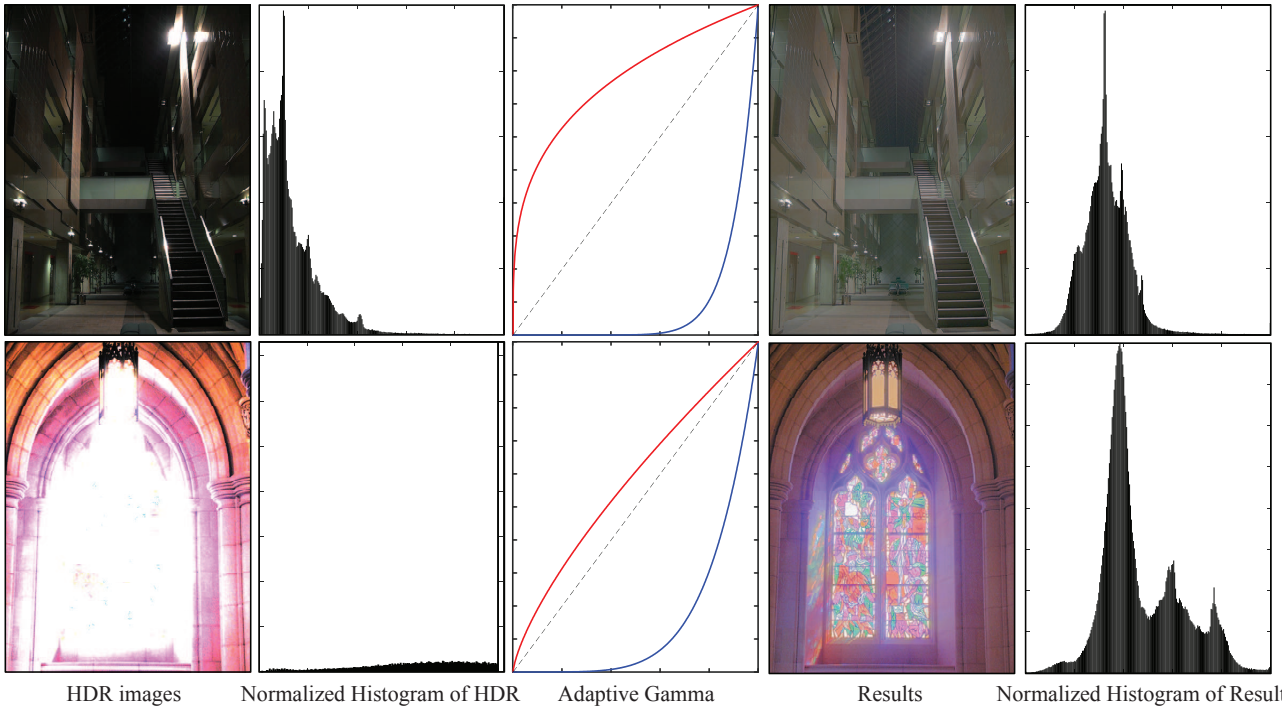

Fig. 3. Two examples with adaptive Gamma correction. The automatically selected red and blue Gamma curves can improve the visibility of dark and bright regions, respectively. Note that the histograms are obtained from luminance channels of the corresponding scenes.

Fig. 4. Color restoration results with specific s values (in (15)) and the results with the proposed luminance-dependant adaptive s.

of bright regions, while a red curve with γ value close to 1.0 is selected to almost neglect the enhancement of dark regions. Totally, our method can select suitable Gamma curves according to the luminance distribution of the given scene to achieve adaptive dynamic range adjustment and enhance the overall visibility of the image details.

In addition, we also analyzed the influence of the parameter s in (15) for color saturation restoration. Fig.4 shows an example of color restoration results with different fixed s values and the proposed luminance-dependant spatially varying s. We can clearly see that a smaller s will make the recovered image under-saturated, while the recovered image with a larger s will be over-saturated. In contrast, the adaptive s used in this work (16) can provide a good balance between the visible naturalness and the consistence to the original color.

B. HDR compression and enhancement

In this experiment, we first estimated our method on the HDR dynamic compression task. The results of comparisons with the Retinex-based methods, including Meylan's adaptive Retinex [15] and MSRCR [14], are listed in Fig.5. The results of Meylan's method were obtained by running the original codes from the authors. From the visual comparison, we can see that Meylan's method usually leads to color shift especially when the scene contains monotonous predominant color (see the first row). In contrast, the proposed method obtains more natural color (see the first and second rows) and clearer details in both of the dark and bright regions (see the bottom row for an example) in comparison to the results of Meylan's method and MSRCR.

Fig. 6 shows several scenes that were obtained at differ-

1051-8215 (c) 2018 IEEE. Personal use is permitted, but republication/redistribution requires IEEE permission. See http://www.ieee.org/publications_standards/publications/rights/index.html for more information.

This article has been accepted for publication in a future issue of this journal, but has not been fully edited. Content may change prior to final publication. Citation information: DOI 10.1109/TCSVT.2018.2810212, IEEE Transactions on Circuits and Systems for Video Technology

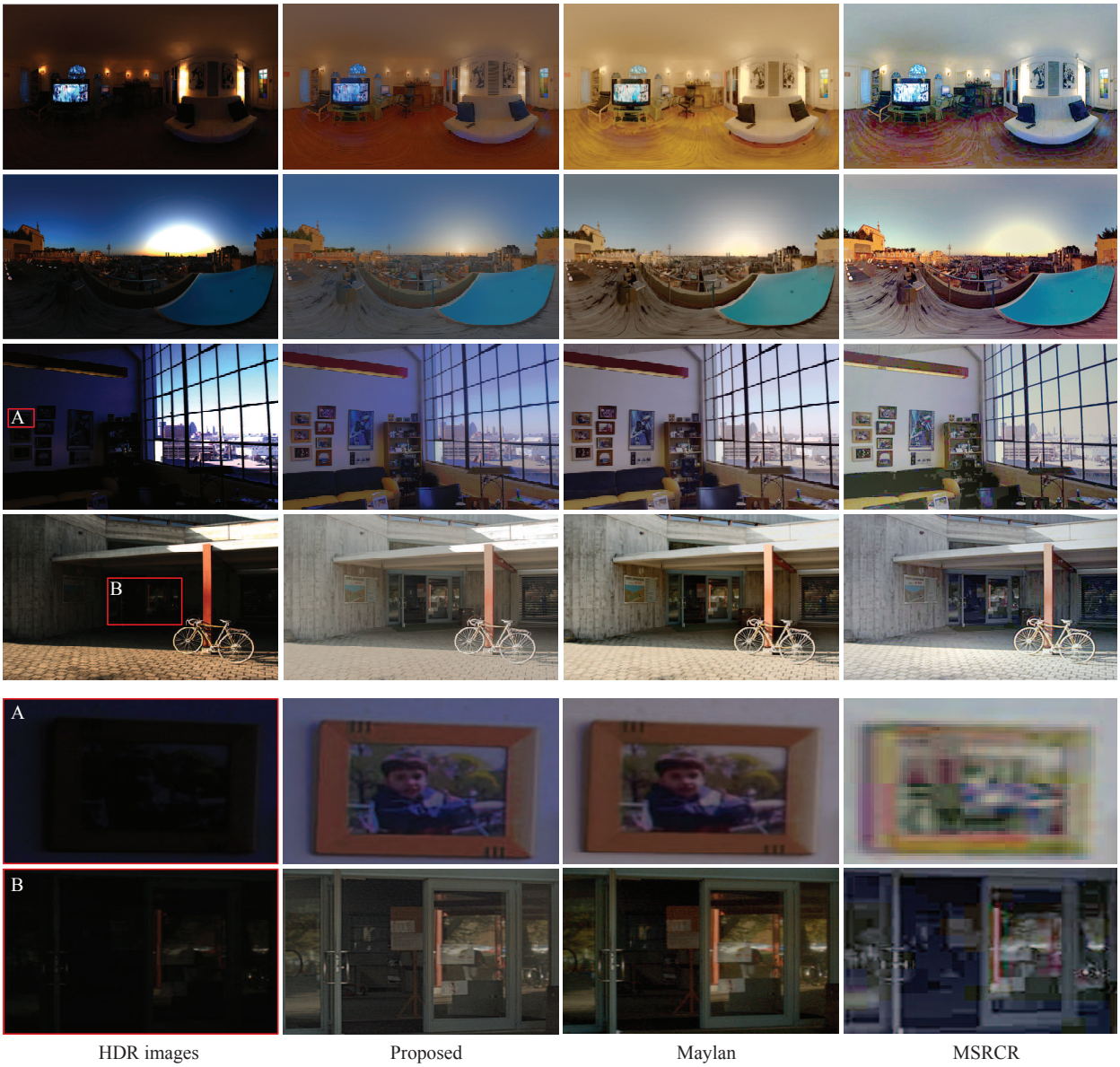

Fig. 5. Comparison of the HDR tone mapping results with the Retinex-based methods, including Meylan's adaptive Retinex [15] and MSRCR [14].

ent exposure levels, downloaded from http://www.empamedia.ethz.ch/hdrdatabase/index.php, for more visual comparisons. Generally speaking, the proposed method can well balance the details of under-exposed regions and over-exposed regions. From Fig. 6, the results of our method have similar luminance range with the mid-exposed scenes, but more clear details in the dark regions.

In addition, we evaluated our results on the image set collected by Yeganeh and Wang [58], which contains 15 HDR scenes and subjective scores on the results of 8 typical TM methods, including the methods developed by Reinhard *et al*. [5], Drago *et al*. [4], Durand and Dorsey [19], Mantiuk *et al*. [61] and Pattanaik *et al*. [62] and "Exposure and Gamma", "Equalize Histogram", and "Local Adaptation" in Adobe Photoshop. Because Yeganeh and Wang named these eight methods with number '1' to '8' in their dataset, we also correspondingly name these methods with 'M1' to 'M8" instead of the specific method's name to avoid mismatching. In order to clearly demonstrate the performance, we compare our results in Fig. 7 with the best three ones among the eight methods provided by [58], in which M7, M6 and M2 obtain the highest scores with quantitative metrics in Fig. 8 and achieve the best subjective evaluation (data is provided by [58]). In Fig. 7, the number at the lower-right corner in each scene is the Mean Opinion Score (MOS) (lower is better [58]), and the best results among the compared methods are marked by the red boxes. We can clearly see that the best scores are achieved by different methods for different scenes, and the visual quality of final images by our method is closer to the best results among the compared methods.

In order to further estimate the TM performance in a quantitative way, we employed several metrics to evaluate the proposed method and the compared methods. Tone-mapped image quality index (TMQI) is a recent metric to assess

1051-8215 (c) 2018 IEEE. Personal use is permitted, but republication/redistribution requires IEEE permission. See http://www.ieee.org/publications_standards/publications/rights/index.html for more information.

This article has been accepted for publication in a future issue of this journal, but has not been fully edited. Content may change prior to final publication. Citation information: DOI 10.1109/TCSVT.2018.2810212, IEEE Transactions on Circuits and Systems for Video Technology

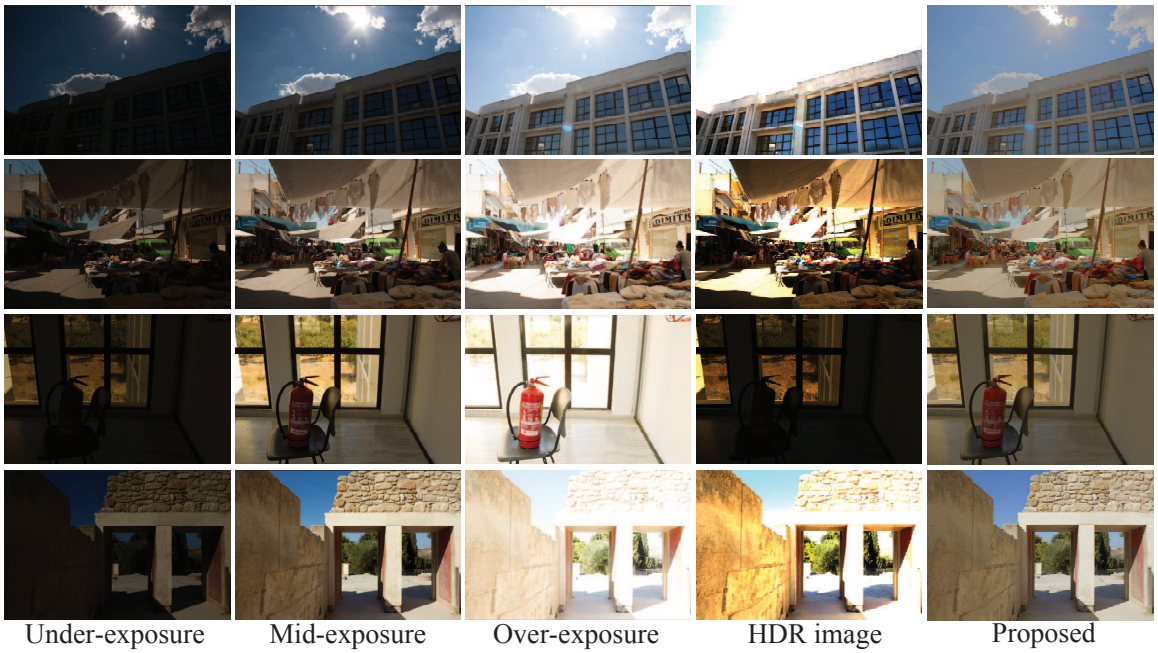

Fig. 6. Comparison of our TM results with the images captured at different exposure levels.

TABLE I
MEAN COMPUTATION TIME(IN SECOND) ON THE 15 SCENES COLLECTED BY [58]. THE COMPUTER USED HERE IS INTER I7-6700K, 4.0GHZ WITH 16.0G RAM.

Durand *et al.* [19]	Reinhard *et al.* [5]	Meylan *et al.* [15]	**Proposed**
0.0930	0.2510	32.6403	**1.5240**

the TM methods by considering the structure similarity and naturalness between the maps before and after tone mapping [58]. Considering that the proposed method is mainly aimed to enhance the details of HDR images, we also computed the multi-scale signal fidelity measure on the basis of a modified structural similarity index [58]. Besides, the visibility metric named HDR-VDP-2 [59] was also used for complementary performance evaluation. Fig. 8 lists the TMQI, Structural Fidelity, and HDR-VDP-2 metrics of all compared methods on two datasets: the MPII dataset and the subject test dataset [58]. From Fig. 8, we can clearly see that each method may obtain different score ranking with various metrics. For example, the method of Ward *et al*. obtains the best score of TMQI on the MPII dataset, but it performs moderately in terms of structural fidelity and HDR-VDP-2 (Fig.8(a)). This suggests that these metrics are not good enough to comprehensively evaluate the performance of HDR tone mapping. Meanwhile, this experiment also illuminates that there is no TM method that can obtain the absolutely best performance than others. However, the proposed method can obtain quite competitive performance in comparison to the compared TM methods and performs quite stable with various metrics on different datasets. Moreover, considering that the proposed method is aimed to enhance details of HDR scenes, our method obtains high structural fidelity but loss a little the visual naturalness.

Generally speaking, compressing dynamic range of HDR image often leads to the loss of local contrast, and an efficient local contrast restoration is of great benefit to the visibility of visual images. In our work, we employ a simple DoG filter to achieve edge sharpening considering the computational efficiency. Fig. 9(a) shows the comparison of TMQI for the results with and without edge sharpening on two datasets [58]. In addition, a visual comparison on two images is also listed in Fig. 9(b) to show the enhancement of local contrast after edge sharpening. From the comparison, edge sharpening can further improve not only the qualitative visual quality but also the qualitative metric (TMQI).

We also tested the performance of our method when using various color space to separate color and luminance information. The dynamic adjustment operator is used to enhance the separated luminance channel while maintain the same color saturation restoration (as indicated in section II-D). Fig. 10 shows the results when using different color spaces, including YC_BC_R, XYZ, and HSV. The XYZ space separates luminance channel (i.e., the Y component) with only a slight difference of coefficients comparing to the YC_BC_R space mentioned in Section II-A, therefore our model still obtains similar good results when using XYZ space. When HSV transform is used to extract the luminance channel (i.e., the V component), our method also obtains acceptable results, but the results appear more under-saturated, especially for the regions with monotonous colors.

In order to show the complexity of the proposed method, we added the comparison of time cost for several classical tone mapping algorithms. Table I lists the mean computation time on the 15 scenes collected by [58]. Comparing to the global methods, our method needs a little more time to search the optimal Gamma values. The frequency-based method proposed by Durand *et al* [19]. also gets high computational efficiency via some special code optimization (e.g., fast bilateral filter-

1051-8215 (c) 2018 IEEE. Personal use is permitted, but republication/redistribution requires IEEE permission. See http://www.ieee.org/publications_standards/publications/rights/index.html for more information.

This article has been accepted for publication in a future issue of this journal, but has not been fully edited. Content may change prior to final publication. Citation information: DOI 10.1109/TCSVT.2018.2810212, IEEE Transactions on Circuits and Systems for Video Technology

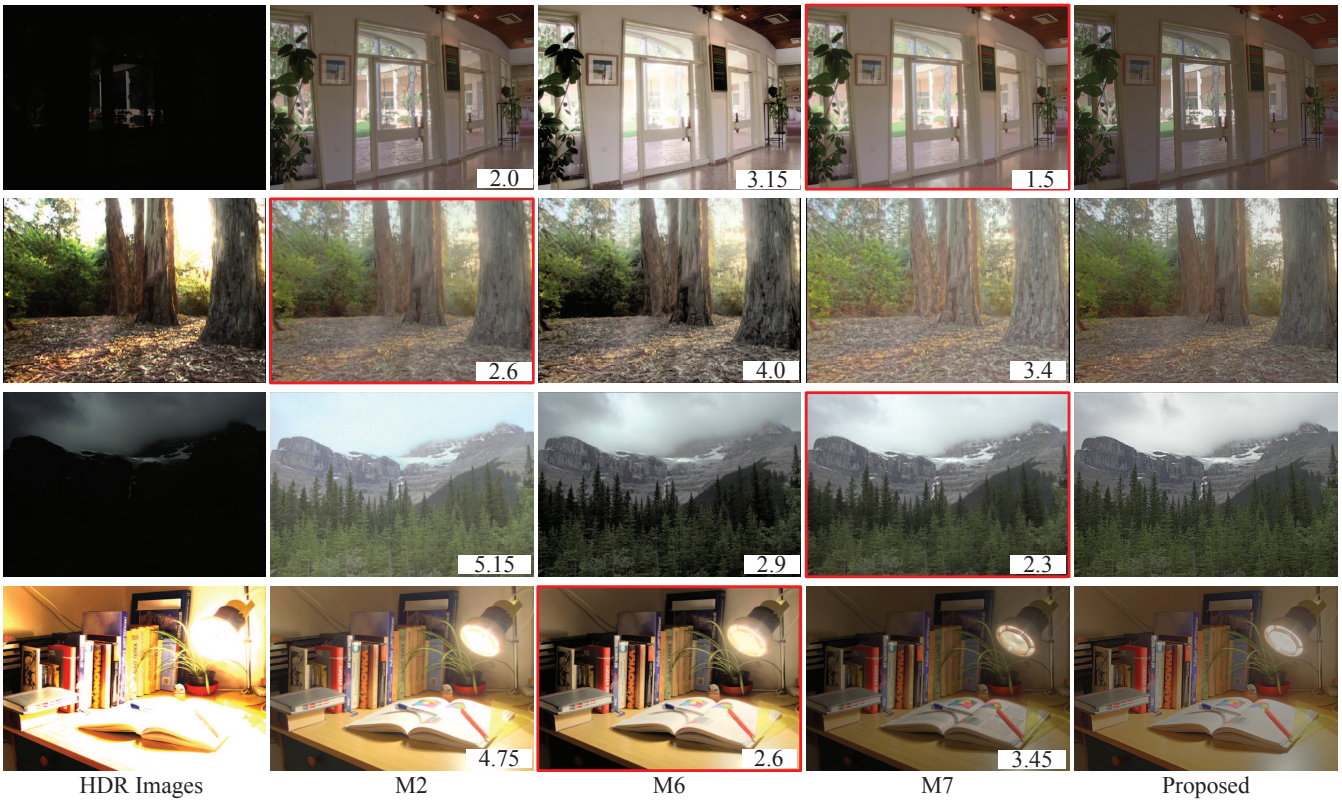

Fig. 7. Comparison of our results with the best three results of several typical TM methods on the dataset provided by [58]. The first column lists the original HDR images, the second to forth columns are the best three results (with the highest subjective scores among the eight methods ('M1' to 'M8' in the text) provided by [58]), and the last column shows the results obtained by our method. The number at the lower-right corner in each scene is the MOS score (lower is better [58]), and the best results among the compared methods are marked by the red boxes.

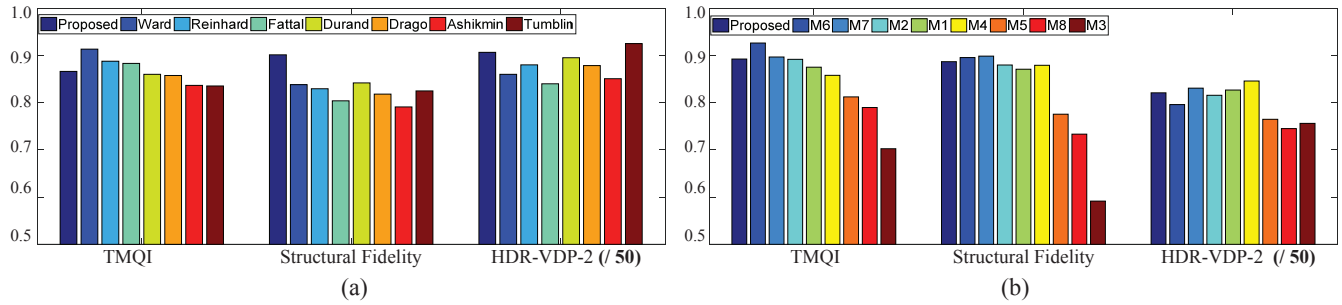

Fig. 8. Comparison of three quantitative metrics estimated on two datasets: (a) MPII scenes and (b) the images collected by [58]. The employed three metrics include TMQI [58], Structural Fidelity [58], and HDR-VDP-2 [59] (which is divided by 50 for convenient display in this figure). The considered methods on the MPII scenes in (a) include the methods proposed by Ward *et al*. [11], Dargo *et al*. [4], Durand *et al*. [19], Reinhard *et al*. [5], and Fattal *et al*. [27], Ashikmin *et al*. [60], Tumblin *et al*. [11]. The methods named as 'M1' to 'M8' in (b) correspond to the eight methods listed in [58] (see the text for details).

ing). However, our method is significantly faster than another adaptive method proposed by Meylan *et al* [15], because the local optimal enhancement in our method is achieved simply by fusing the two corrected images with pixel-wised weights.

C. Nighttime image enhancement and its application

In order to demonstrate the performance in LDR image enhancement, we applied our method in the task of nighttime image enhancement. Considering the particularity of nighttime images (e.g., many dark pixels with intensity close to 0.0), we finely tuned the parameters in our method. First, we revised the (4) and (5) as $M_L = 1/3 + 0.5\sigma_L$ and $M_H = 1 - 0.5\sigma_H$, respectively, to avoid the over-enhancement considering that lots of noises widely present in night images. In addition, we excluded the pixels with the values low than 0.1 when computing the median of Gamma corrected images (in (6)) to search a suitable γ_L, because lots of dark pixels with intensity close to 0.0 will bias the estimate of γ_L.

Fig. 11 shows the night image enhancement results of multiple methods, which are from [66]. The HE method obtains good results for complicated scenes (e.g., the first row), but shows poor performance for scenes with simple background (e.g., the last row). The Gamma correction (GC) method with single (global) Gamma transform usually leads

1051-8215 (c) 2018 IEEE. Personal use is permitted, but republication/redistribution requires IEEE permission. See http://www.ieee.org/publications_standards/publications/rights/index.html for more information.

This article has been accepted for publication in a future issue of this journal, but has not been fully edited. Content may change prior to final publication. Citation information: DOI 10.1109/TCSVT.2018.2810212, IEEE Transactions on Circuits and Systems for Video Technology

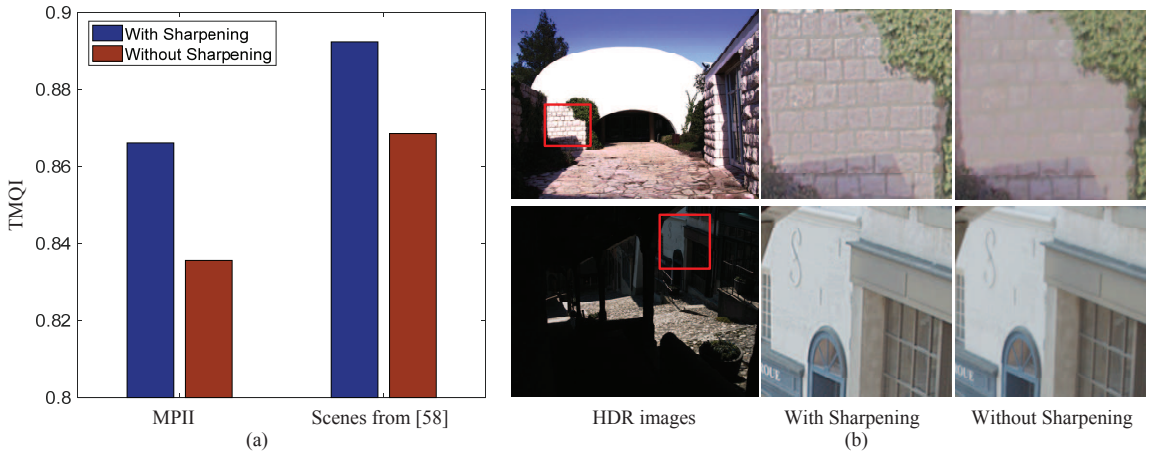

Fig. 9. Evaluating the performance of the proposed method with and without edge sharpening. (a) TMQI estimated on MPII scenes and the images collected by [58]. (b) Two example images illustrating that the edge sharpening operator can improve the local contrast.

Fig. 10. The example results of the proposed method when using various color spaces to separate the color and luminance channels.

to low local contrast. A recent bio-inspired method performs well for night image enhancement [63], but it exhibits over-saturated when the scene is lighten by color light sources. Other method like Dong's method has the similar problem and over-enhances the simple scenes [65]. In contrast, our method can balance the operations of brightness adjustment, local contrast enhancement and color recovery.

The related method proposed in [64] describes an interesting strategy to search an adaptive Gamma for each local image patch based on the statistic features (e.g., histogram) which are trained on nine standard images. Basically, the key idea of both our method and the method in [64] is to select an optimal Gamma value for each pixel of local regions. However, the method in [64] estimates the Gamma values locally based on the feature marching with the sliding window operator, which is time consuming (taking about 170.0s for a 512×512 scene with our re-implemented MATLAB code). In contrast, we take a totally different strategy to obtain local Gamma correction. In our work, we globally search two appropriate Gamma values to correct the given image, while the local optimal Gamma enhancement is achieved by fusing the two corrected images with the luminance-dependant and pixel-wised weights. Therefore, the proposed method (taking about only 1.0s for a 512×512 scene) is significantly faster than the local Gamma estimation in [64]. Fig. 11 also shows the comparison of various methods including the results of our re-implemented adaptive Gamma based method in [64] (denoted by AG) with the same color restoration step in our paper.

It is quite challenging to quantitatively evaluate the performance of various image enhancement methods. In this work, we added an experiment to indirectly estimate the performance of the proposed method. We believe that an efficient image enhancement method as a preprocessing step should substantially contribute to the higher visual tasks, like object detection. Following the work presented in [63], we tested the contribution of our enhancement method in the car detection task of nighttime traffic scenes. In this experiment, some existing frameworks [63], [67] were employed to implement the car detection task. We compared the performance when implementing the car detection on the original night scenes and the enhanced night scenes by our proposed method.

The nighttime vehicle dataset was developed in [67], which can be downloaded from: www.carlib.net/?page_id=35. This dataset includes 450 positive samples and 2000 negative samples in the training set, and 750 negative samples and 1000 positive samples in the test set, and 400 pictures containing

1051-8215 (c) 2018 IEEE. Personal use is permitted, but republication/redistribution requires IEEE permission. See http://www.ieee.org/publications_standards/publications/rights/index.html for more information.

This article has been accepted for publication in a future issue of this journal, but has not been fully edited. Content may change prior to final publication. Citation information: DOI 10.1109/TCSVT.2018.2810212, IEEE Transactions on Circuits and Systems for Video Technology

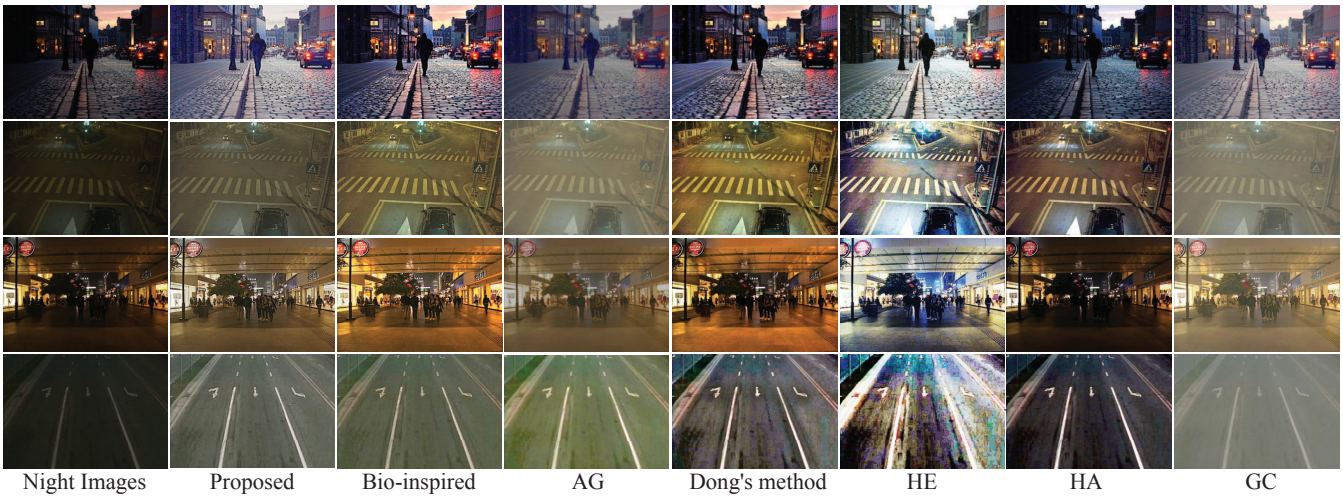

Fig. 11. Night image enhancement results of multiple methods. The first column lists the original images, and the second to eighth columns show the results of the proposed method, a bio-inspired method [63], adaptive Gamma (AG) [64], Dong's method [65], and the results of three classical global methods: histogram equalization (HE), histogram adjustment (HA) and Gamma correction (GC).

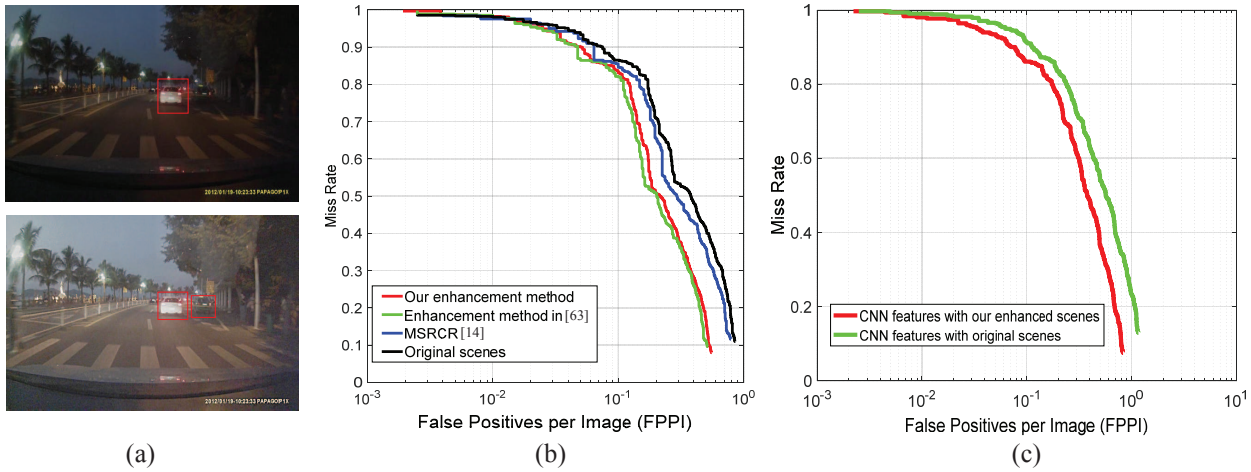

Fig. 12. Illustration of the proposed method contributing to higher object(car) detection tasks. (a) an example showing that one car is missed in the original scene due to the quite low contrast (top), but the two cars (marked by red boxes) are correctly detected when using the enhanced scenes (bottom). (b) The curves of the miss rate Vs. false positives per image for different image enhancement methods using the basic LBP and HOG features. (c) The curves illustrating that our enhancement method also contributes to the following object detection even with robust pre-trained CNN features.

634 vehicles in the detection set. Fig. 12(a) shows an example that one car is missed in the original night scene due to the quite low contrast; but that car is correctly detected after the scene is enhanced by our method. Fig. 12(b) shows the curves of the miss rate versus false positives per image for different image enhancement methods using the basic features of local binary patterns (LBP) and histogram of oriented gradients (HOG) used in [63]. This figure illustrates that the proposed image enhancement method can facilitate the task of car detection in night traffic scenes. Our method obtains similar performance as the bio-inspired enhancement method in [63] and outperforms the classical MSRCR method [14], and shows the lowest miss rate over all detection images (see the end point of each curves). This comparison evaluates our proposed method is very effective for nighttime car vehicle detection task. Another comparison using the pre-trained convolutional neural networks (CNN) features [68] is shown in Fig. 12(c), which illustrates that a good image enhancement method can clearly contribute to the following task of object detection even using the robust CNN features. For a specific object detection task, there is no sufficient labeled training data for CNN feature learning, thus an efficient image preprocessing operator (e.g., image enhancement) can efficiently improve the performance when using the pre-trained CNN model on the general enormous labeled dataset.

IV. Conclusion and Discussion

In this paper, we proposed an efficient flowchart for image dynamic range adjustment by employing adaptive Gamma correction, image fusion and luminance-dependant color restoration. The proposed method was comprehensively evaluated for the tasks of HDR tone mapping and LDR nighttime image enhancement. The experimental results demonstrate that the proposed method obtains quite competitive performance in

1051-8215 (c) 2018 IEEE. Personal use is permitted, but republication/redistribution requires IEEE permission. See http://www.ieee.org/publications_standards/publications/rights/index.html for more information.

This article has been accepted for publication in a future issue of this journal, but has not been fully edited. Content may change prior to final publication. Citation information: DOI 10.1109/TCSVT.2018.2810212, IEEE Transactions on Circuits and Systems for Video Technology

tone mapping of HDR scenes with good detail enhancement and structure protection. In addition, the experimental results on LDR night image enhancement also suggest that the proposed method can clearly contribute to the tasks of car detection in complex night scenes. Facing the numerous methods that have been developed for dynamic range adjustment, we hope that the present work makes contribution to this field by providing inspiration in improving the existing tone mapping methods with the proposed simple yet efficient strategies of adaptive operations. In addition, the proposed adaptive fusion and color restoration methods may also be incorporated into the pipeline of creating HDR images of the digital cameras or videos.

Note that as a general image enhancement method, our method focuses on improving the visibility of details in low quality scenes. For HDR images, the dynamic range compression may lead to a little loss of visual naturalness. Moreover, night images usually suffer from serious noises, and most image enhancement operators may also amplify the noises. Therefore, as one of our future works, introducing some more flexible non-linear transformations and more efficient adaptation mechanisms are expected to further improve the robustness of the proposed method. In addition, some denoising mechanisms can also be integrated into the current framework in the future to suppress noises and improve the visual naturalness of the enhanced images.

REFERENCES

[1] E. Reinhard, W. Heidrich, P. Debevec, S. Pattanaik, G. Ward, and K. Myszkowski, *High dynamic range imaging: acquisition, display, and image-based lighting*. Morgan Kaufmann, 2010.

[2] G. Miller and C. R. Hoffman, "Illumination and reflection maps: Simulated objects in simulated and real environments," in *SIGGRAPH'84 Advanced Computer Graphics Animation seminar notes*, vol. 190, 1984.

[3] J. Tumblin and G. Turk, "LCIS: A boundary hierarchy for detail-preserving contrast reduction," in *Proc. Conf. Computer Graphics and Interactive Techniques*. ACM Press/Addison-Wesley Publishing Co., 1999, pp. 83–90.

[4] F. Drago, K. Myszkowski, T. Annen, and N. Chiba, "Adaptive logarithmic mapping for displaying high contrast scenes," in *Computer Graphics Forum*, vol. 22, no. 3. Wiley Online Library, 2003, pp. 419–426.

[5] E. Reinhard, M. Stark, P. Shirley, and J. Ferwerda, "Photographic tone reproduction for digital images," *ACM Trans. Graphics*, vol. 21, no. 3, pp. 267–276, 2002.

[6] J. E. Dowling, *The retina: an approachable part of the brain*. Harvard University Press, 1987.

[7] C. Schlick, "Quantization techniques for visualization of high dynamic range pictures," in *Photorealistic Rendering Techniques*. Springer, 1995, pp. 7–20.

[8] S. N. Pattanaik, J. A. Ferwerda, M. D. Fairchild, and D. P. Greenberg, "A multiscale model of adaptation and spatial vision for realistic image display," in *Proc. Ann. Conf. Computer Graphics and Interactive Techniques*. ACM, 1998, pp. 287–298.

[9] J. Tumblin, J. K. Hodgins, and B. K. Guenter, "Two methods for display of high contrast images," *ACM Trans. Graphics*, vol. 18, no. 1, pp. 56–94, 1999.

[10] Y. Li, X. Pu, H. Li, and C. Li, "A retinal adaptation model for hdr image compression," in *Perception*, vol. 45. Sage Publications Ltd 1 Olivers Yard, 55 City Road, London Ec1y 1sp, England, 2016, pp. 45–45.

[11] G. Ward, "A contrast-based scalefactor for luminance display," *Graphics gems IV*, pp. 415–421, 1994.

[12] E. H. Land and J. J. McCann, "Lightness and retinex theory," *Journal of the Optical Society of America A: Optics, Image Science & Vision*, vol. 61, no. 1, pp. 1–11, 1971.

[13] D. J. Jobson, Z.-u. Rahman, and G. A. Woodell, "Properties and performance of a center/surround retinex," *IEEE Trans. Image Process.*, vol. 6, no. 3, pp. 451–462, 1997.

[14] D. J. Jobson, Z.-u. Rahman, and G. A. Woodell, "A multiscale retinex for bridging the gap between color images and the human observation of scenes," *IEEE Trans. Image Process.*, vol. 6, no. 7, pp. 965–976, 1997.

[15] L. Meylan and S. Susstrunk, "High dynamic range image rendering with a retinex-based adaptive filter," *IEEE Trans. Image Process.*, vol. 15, no. 9, pp. 2820–2830, 2006.

[16] S. Lee, "An efficient content-based image enhancement in the compressed domain using retinex theory," *IEEE Trans. Circuits Syst. Video Technol.*, vol. 17, no. 2, pp. 199–213, 2007.

[17] S. Gao, W. Han, Y. Ren, and Y. Li, "High dynamic range image rendering with a luminance-chromaticity independent model," in *Proc. Int. Conf. Intell. Science and Big Data Engineering*. Springer, 2015, pp. 220–230.

[18] S. Pattanaik and H. Yee, "Adaptive gain control for high dynamic range image display," in *Proc. Spring Conf. Computer Graphics*. ACM, 2002, pp. 83–87.

[19] F. Durand and J. Dorsey, "Fast bilateral filtering for the display of high-dynamic-range images," in *ACM Trans. Graphics*, vol. 21, no. 3. ACM, 2002, pp. 257–266.

[20] Y. H. Yee and S. Pattanaik, "Segmentation and adaptive assimilation for detail-preserving display of high-dynamic range images," *The Visual Computer*, vol. 19, no. 7, pp. 457–466, 2003.

[21] X.-S. Zhang and Y.-J. Li, "A retina inspired model for high dynamic range image rendering," in *Proc. Int. Conf. Brain Inspired Cognit. Syst.* Springer, 2016, pp. 68–79.

[22] A. v. Oppenheim, R. Schafer, and T. Stockham, "Nonlinear filtering of multiplied and convolved signals," *IEEE Trans. Audio and Electroacoustics*, vol. 16, no. 3, pp. 437–466, 1968.

[23] P. Choudhury and J. Tumblin, "The trilateral filter for high contrast images and meshes," in *ACM SIGGRAPH Courses*. ACM, 2005, p. 5.

[24] K. He, J. Sun, and X. Tang, "Guided image filtering," *IEEE Trans. Pattern. Anal. Mach. Intell.*, vol. 35, no. 6, pp. 1397–1409, 2013.

[25] Z. Li, J. Zheng, Z. Zhu, W. Yao, and S. Wu, "Weighted guided image filtering," *IEEE Trans. Image process.*, vol. 24, no. 1, pp. 120–129, 2015.

[26] Z. Farbman, R. Fattal, D. Lischinski, and R. Szeliski, "Edge-preserving decompositions for multi-scale tone and detail manipulation," in *ACM Trans. Graphics*, vol. 27, no. 3. ACM, 2008, p. 67.

[27] R. Fattal, D. Lischinski, and M. Werman, "Gradient domain high dynamic range compression," in *ACM Trans. Graphics*, vol. 21, no. 3. ACM, 2002, pp. 249–256.

[28] R. C. Gonzalez and R. E. Woods, "Image processing," *Digital Image Process.*, vol. 2, 2007.

[29] J.-Y. Kim, L.-S. Kim, and S.-H. Hwang, "An advanced contrast enhancement using partially overlapped sub-block histogram equalization," *IEEE Trans. Circuits Syst. Video Technol.*, vol. 11, no. 4, pp. 475–484, 2001.

[30] T. Arici, S. Dikbas, and Y. Altunbasak, "A histogram modification framework and its application for image contrast enhancement," *IEEE Trans. Image Process.*, vol. 18, no. 9, pp. 1921–1935, 2009.

[31] H.-D. Liu, M. Yang, Y. Gao, and L. Cao, "Fast local histogram specification," *IEEE Trans. Circuits Syst. Video Technol.*, vol. 24, no. 11, pp. 1833–1843, 2014.

[32] H. Xu, G. Zhai, X. Wu, and X. Yang, "Generalized equalization model for image enhancement," *IEEE Trans. Multimedia*, vol. 16, no. 1, pp. 68–82, 2014.

[33] Y.-T. Kim, "Contrast enhancement using brightness preserving bi-histogram equalization," *IEEE Trans. Consumer Elect.*, vol. 43, no. 1, pp. 1–8, 1997.

[34] T. K. Kim, J. K. Paik, and B. S. Kang, "Contrast enhancement system using spatially adaptive histogram equalization with temporal filtering," *IEEE Trans. Consumer Elect.*, vol. 44, no. 1, pp. 82–87, 1998.

[35] A. R. Rivera, B. Ryu, and O. Chae, "Content-aware dark image enhancement through channel division," *IEEE Trans. Image Process.*, vol. 21, no. 9, pp. 3967–3980, 2012.

[36] K. Gu, G. Zhai, X. Yang, W. Zhang, and C. W. Chen, "Automatic contrast enhancement technology with saliency preservation," *IEEE Trans. Circuits Syst. Video Technol.*, vol. 25, no. 9, pp. 1480–1494, 2015.

[37] C. Jung and T. Sun, "Optimized perceptual tone mapping for contrast enhancement of images," *IEEE Trans. Circuits Syst. Video Technol.*, vol. 27, no. 6, pp. 1161–1170, 2017.

[38] W.-M. Ke, C.-R. Chen, and C.-T. Chiu, "BiTA/SWCE: Image enhancement with bilateral tone adjustment and saliency weighted contrast enhancement," *IEEE Trans. Circuits Syst. Video Technol.*, vol. 21, no. 3, pp. 360–364, 2011.

[39] Y. Chen, W. Lin, C. Zhang, Z. Chen, N. Xu, and J. Xie, "Intra-and-inter-constraint-based video enhancement based on piecewise tone mapping," *IEEE Trans. Circuits Syst. Video Technol.*, vol. 23, no. 1, pp. 74–82, 2013.

1051-8215 (c) 2018 IEEE. Personal use is permitted, but republication/redistribution requires IEEE permission. See http://www.ieee.org/publications_standards/publications/rights/index.html for more information.

This article has been accepted for publication in a future issue of this journal, but has not been fully edited. Content may change prior to final publication. Citation information: DOI 10.1109/TCSVT.2018.2810212, IEEE Transactions on Circuits and Systems for Video Technology

[40] V. Naidu and J. Raol, "Pixel-level image fusion using wavelets and principal component analysis," *Defence Science Journal*, vol. 58, no. 3, p. 338, 2008.

[41] A. Saleem, A. Beghdadi, and B. Boashash, "Image fusion-based contrast enhancement," *EURASIP J. Image Video Process.*, vol. 2012, no. 1, p. 10, 2012.

[42] R. Mantiuk, S. Daly, and L. Kerofsky, "Display adaptive tone mapping," in *ACM Trans. Graphics*, vol. 27, no. 3. ACM, 2008, p. 68.

[43] Z. Mai, H. Mansour, R. Mantiuk, P. Nasiopoulos, R. Ward, and W. Heidrich, "Optimizing a tone curve for backward-compatible high dynamic range image and video compression," *IEEE Trans. Image Process.*, vol. 20, no. 6, pp. 1558–1571, 2011.

[44] D. Baylor and M. Fuortes, "Electrical responses of single cones in the retina of the turtle," *The Journal of physiology*, vol. 207, no. 1, pp. 77–92, 1970.

[45] R. Boynton and D. Whitten, "Visual adaptation in monkey cones: recordings of late receptor potentials," *Science*, vol. 170, no. 3965, pp. 423–1426, 1970.

[46] S. G. Solomon and A. Kohn, "Moving sensory adaptation beyond suppressive effects in single neurons," *Current Biology*, vol. 24, no. 20, pp. R1012–R1022, 2014.

[47] M. Carandini and D. J. Heeger, "Normalization as a canonical neural computation," *Nature Reviews Neuroscience*, vol. 13, no. 1, pp. 51–62, 2012.

[48] J. Shen, Y. Zhao, S. Yan, X. Li *et al.*, "Exposure fusion using boosting laplacian pyramid." *IEEE Trans. Cybernetics*, vol. 44, no. 9, pp. 1579–1590, 2014.

[49] A. A. Goshtasby, "Fusion of multi-exposure images," *Image and Vision Computing*, vol. 23, no. 6, pp. 611–618, 2005.

[50] M. A. Robertson, S. Borman, and R. L. Stevenson, "Dynamic range improvement through multiple exposures," in *Proc. Int. Conf. Image Process.*, vol. 3. IEEE, 1999, pp. 159–163.

[51] Z. Li and J. Zheng, "Single image brightening via exposure fusion," in *Proc. IEEE Int. Conf. Acoustics, Speech and Signal Processing*. IEEE, 2016, pp. 1756–1760.

[52] Z. Li, Z. Wei, C. Wen, and J. Zheng, "Detail-enhanced multi-scale exposure fusion," *IEEE Trans. Image Process.*, vol. 26, no. 3, pp. 1243–1252, 2017.

[53] A. Gijsenij, T. Gevers, and J. Van De Weijer, "Computational color constancy: Survey and experiments," *IEEE Trans. Image Process.*, vol. 20, no. 9, pp. 2475–2489, 2011.

[54] K.-F. Yang, S.-B. Gao, and Y.-J. Li, "Efficient illuminant estimation for color constancy using grey pixels," in *Proc. IEEE Conf. Comput. Vision Pattern Recognit.* IEEE, 2015, pp. 2254–2263.

[55] S.-B. Gao, K.-F. Yang, C.-Y. Li, and Y.-J. Li, "Color constancy using double-opponency," *IEEE Trans. Pattern. Anal. Mach. Intell.*, vol. 37, no. 10, pp. 1973–1985, 2015.

[56] R. Hall, *Illumination and color in computer generated imagery*. Springer Science & Business Media, 2012.

[57] R. Mantiuk, A. Tomaszewska, and W. Heidrich, "Color correction for tone mapping," in *Computer Graphics Forum*, vol. 28, no. 2. Wiley Online Library, 2009, pp. 193–202.

[58] H. Yeganeh and Z. Wang, "Objective quality assessment of tone-mapped images," *IEEE Trans. Image Process.*, vol. 22, no. 2, pp. 657–667, 2013.

[59] R. Mantiuk, K. J. Kim, A. G. Rempel, and W. Heidrich, "HDR-VDP-2: a calibrated visual metric for visibility and quality predictions in all luminance conditions," in *ACM Trans. Graphics*, vol. 30, no. 4. ACM, 2011, p. 40.

[60] M. Ashikhmin, "A tone mapping algorithm for high contrast images," in *Proc. Eurographics Workshop on Rendering*. Eurographics Association, 2002, pp. 145–156.

[61] R. Mantiuk, K. Myszkowski, and H.-P. Seidel, "A perceptual framework for contrast processing of high dynamic range images," *ACM Trans. Applied Perception*, vol. 3, no. 3, pp. 286–308, 2006.

[62] S. N. Pattanaik, J. Tumblin, H. Yee, and D. P. Greenberg, "Time-dependent visual adaptation for fast realistic image display," in *Proc. Ann. Conf. Computer Graphics and Interactive Techniques*. ACM Press/Addison-Wesley Publishing Co., 2000, pp. 47–54.

[63] H. Kuang, X. Zhang, Y.-J. Li, L. L. H. Chan, and H. Yan, "Nighttime vehicle detection based on bio-inspired image enhancement and weighted score-level feature fusion," *IEEE Trans. Intell. Transport. Syst.*, vol. 18, no. 4, pp. 927–936, 2017.

[64] M. FarshbafDoustar and H. Hassanpour, "A locally-adaptive approach for image gamma correction," in *Proc. Int. Conf. Information Sciences Signal Processing and their Applications*. IEEE, 2010, pp. 73–76.

[65] X. Dong, G. Wang, Y. Pang, W. Li, J. Wen, W. Meng, and Y. Lu, "Fast efficient algorithm for enhancement of low lighting video," in *Proc. IEEE Int. Conf. Multimedia and Expo*. IEEE, 2011, pp. 1–6.

[66] Z. Chen, T. Jiang, and Y. Tian, "Quality assessment for comparing image enhancement algorithms," in *Proc. IEEE Conf. Comput. Vision Pattern Recognit.*, 2014, pp. 3003–3010.

[67] H. Kuang, L. Chen, F. Gu, J. Chen, L. Chan, and H. Yan, "Combining region-of-interest extraction and image enhancement for nighttime vehicle detection," *IEEE Intell. Syst.*, vol. 31, no. 3, pp. 57–65, 2016.

[68] P. Sermanet, D. Eigen, X. Zhang, M. Mathieu, R. Fergus, and Y. LeCun, "Overfeat: Integrated recognition, localization and detection using convolutional networks," *arXiv preprint arXiv:1312.6229*, 2013.

Kai-Fu Yang received the Ph.D. degree in biomedicalengineering from the University of Electronic Science and Technology of China (UESTC), Chengdu, China, in 2016. He is currently an associate professor with the MOE Key Lab for Neuroinformation, School of Life Science and Technology, UESTC, Chengdu, China. His research interests include cognitive computing and brain-inspired computer vision.

Hui Li received a Master degree in Biomedical engineering from University of Electronic Science and Technology of China, Chengdu, China, in 2016. Her research interests include visual mechanism modeling and image processing.

Hulin Kuang received the M. Eng. and B. Eng. degree in Wuhan University, China in 2013 and 2011 respectively. He obtained PhD degree in City University of Hong Kong in 2016. Now he is a postdoc of Department of Clinical Neurosciences, University of Calgary, Canada. His current research interests include image processing, computer vision and pattern recognition.

Chao-Yi Li received the degrees from Chinese Medical University, Shenyang, China, in 1956, and Fudan University, Shanghai, China, in 1961. He is currently a Professor with the University of Electronic Science and Technology of China, Chengdu, China, and the Shanghai Institutes for Biological Sciences, Chinese Academy of Sciences. His research interest is mainly in visual neurophysiology.

Yong-Jie Li (M'14-SM'16) received the Ph.D. degree in biomedical engineering from the University of Electronic Science and Technology of China (UESTC), Chengdu, China, in 2004. He is currently a Professor with the MOE Key Lab for Neuroinformation, School of Life Science and Technology, UESTC. His research interests include visual mechanism modeling, image processing, and intelligent computation.

1051-8215 (c) 2018 IEEE. Personal use is permitted, but republication/redistribution requires IEEE permission. See http://www.ieee.org/publications_standards/publications/rights/index.html for more information.